The Canadian Mineralogist
Vol. 38, pp. 1477-1485 (2000)

GLADIUSITE, $Fe^{3+}_2(Fe^{2+},Mg)_4(PO_4)(OH)_{11}(H_2O)$, A NEW HYDROTHERMAL MINERAL SPECIES FROM THE PHOSCORITE–CARBONATITE UNIT, KOVDOR COMPLEX, KOLA PENINSULA, RUSSIA

RUSLAN P. LIFEROVICH¶

Institute of Geosciences, University of Oulu, PL 8000, FIN-90401 Oulu, Finland

ELENA V. SOKOLOVA‡ AND FRANK C. HAWTHORNE§

Department of Geological Sciences, University of Manitoba, Winnipeg, Manitoba R3T 2N2, Canada

KAUKO V.O. LAAJOKI AND SEPPO GEHÖR

Institute of Geosciences, University of Oulu, PL 8000, FIN-90401 Oulu, Finland

YAKOV A. PAKHOMOVSKY AND NATALY V. SOROKHTINA

Geological Institute, Kola Science Center, Russian Academy of Sciences, Apatity 184200, Russia

Abstract

Gladiusite, ideally $Fe^{3+}_2(Fe^{2+},Mg)_4(PO_4)(OH)_{11}(H_2O)$, monoclinic, *a* 16.959(2), *b* 11.650(3), *c* 6.266(6) Å, β 90.00(5)°, *V* 1238(1) Å^3, space group $P2_1/n$, $Z = 4$, is a new mineral species from hydrothermal assemblages associated with the phoscorite–carbonatite unit of the Kovdor alkaline-ultramafic complex, Kola Peninsula, Russia. It occurs in vugs within veins of mineralized dolomite carbonatite. Associated minerals are dolomite, pyrochlore, several generations of magnetite, pyrite, rutile, a ternovite-like phase, catapleiite, bobierrite, rimkorolgite, juonniite, strontiowhitlockite, collinsite (including a Sr-rich variety) and chlorite. Gladiusite occurs as acicular aggregates and as free-standing radial clusters (<2 mm in diameter) of arrow-headed crystals. Acicular crystals vary from 0.5 to 6–7 μm thick and from 10 to 500 μm long. Gladiusite is dark green, almost black, with an olive-green streak, opaque in aggregates and translucent in thin crystals; it has a vitreous luster, and does not fluoresce under long- or short-wave ultraviolet light. It has a Mohs hardness of 4–4½, and is brittle with an irregular fracture; cleavage and parting were not observed. The measured and calculated densities are 3.11(2) and 3.10(4) g/cm^3, respectively. Gladiusite is biaxial negative and strongly pleochroic, α 1.722(2), β 1.730(2), γ 1.737(2), $2V_{calc.}$ = 78.3°. The strongest reflections in the X-ray powder-diffraction pattern [*d* in Å(*I*)(*hkl*)] are: 9.61(53)(110), 6.87(77)(210), 5.83(89)(020), 4.805(100)(220), 3.787(62)(130), 3.533(84)(230), and 2.868(66)(140). Electron-microprobe analysis and Mössbauer spectroscopy gave (wt.%) FeO 25.00, Fe_2O_3 29.90, MgO 11.16, MnO 0.78, P_2O_5 12.46, TiO_2 0.04, H_2O(calc.) = 20.18, sum = 99.51 wt.%; the H_2O content, obtained by the Penfield method, is 19.7 wt.%. The unit formula is $Fe^{3+}_{2.00}[Fe^{2+}_{2.02}Mg_{1.61}Fe^{3+}_{0.17}Mn^{2+}_{0.06}]_{\Sigma 3.86}(P_{1.02}O_4)(OH)_{11}(H_2O)$ on the basis of 16 O atoms. The simplified formula is $Fe^{3+}_2(Fe^{2+},Mg)_4(PO_4)(OH)_{11}(H_2O)$. Crystal-structure study showed gladiusite to be extensively twinned on [001]. Gladiusite is considered to be a product of hydrothermal alteration of pyrrhotite and fluorapatite, the primary Fe and P minerals in the dolomite carbonatite. The mineral is named in accordance with the morphology of the crystals, which resemble double-edge swords (*gladius*, in Latin) in SEM images.

Keywords: gladiusite, new mineral species, electron-microprobe analysis, infrared spectrum, thermogravimetric analysis, differential thermal analysis, hydroxy-hydrated phosphate, Kovdor, Russia.

Sommaire

Nous décrivons la gladiusite, dont la formule idéale est $Fe^{3+}_2(Fe^{2+},Mg)_4(PO_4)(OH)_{11}(H_2O)$, nouvelle espèce minérale monoclinique, *a* 16.959(2), *b* 11.650(3), *c* 6.266(6) Å, β 90.00(5)°, *V* 1238(1) Å^3, groupe spatial $P2_1/n$, $Z = 4$, provenant d'un assemblage hydrothermal associé à la phoscorite et la carbonatite du complexe alcalin-ultramafique de Kovdor, péninsule de Kola, en Russie. On la trouve dans des cavités à l'intérieur de veines de carbonatite à dolomite minéralisée. Lui sont associées

§ *E-mail address*: frank_hawthorne@umanitoba.ca
¶ *Permanent address*: Geological Institute, Kola Science Center, Russian Academy of Sciences, Apatity 184200, Russia.
‡ Department of Crystallography and Crystal Chemistry, Moscow State University, Vorob'evy gory, Moscow 119899, Russia.

dolomite, pyrochlore, plusieurs générations de magnétite, pyrite, rutile, une phase ressemblant à la ternovite, catapléiite, bobierrite, rimkorolgite, juonniite, strontiowhitlockite, collinsite (y inclus une variété riche en Sr) et chlorite. La gladiusite se présente en agrégats aciculaires et en groupes fibroradiés (<2 mm en diamètre) de cristaux pointus. Les cristaux aciculaires vont de 0.5 à 6–7 μm en épaisseur et de 10 à 500 μm en longueur. La gladiusite est vert foncé, presque noire, avec une rayure vert-olive, mais elle est opaque en aggrégats et translucide en cristaux plus minces; son éclat est vitreux, et elle ne montre aucune fluorescence en lumière ultra-violette (ondes courtes ou longues). Sa dureté de Mohs est de 4–4½, et elle est cassante, avec une fracture irrégulière. Aucun clivage ou plan de séparation n'a été décelé. La densité mesurée et calculée est égale à 3.11(2) et 3.10(4) g/cm^3, respectivement. La gladiusite est biaxe négative et fortement pléochroïque, α 1.722(2), β 1.730(2), γ 1.737(2), $2V_{calc.}$ = 78.3°. Les sept raies les plus intenses du spectre de diffraction (méthode des poudres) [*d* en Å(*I*)(*hkl*)] sont: 9.61(53)(110), 6.87(77)(210), 5.83(89)(020), 4.805(100)(220), 3.787(62)(130), 3.533(84)(230), et 2.868(66)(140). Une analyse avec une microsonde électronique, supplémentée par un spectre de Mössbauer, ont donné FeO 25.00, Fe_2O_3 29.90, MgO 11.16, MnO 0.78, P_2O_5 12.46, TiO_2 0.04, H_2O(calc.) 20.18, total 99.51% (poids); la proportion de H_2O, mesurée par la méthode de Penfield, est 19.7°. L'unité formulaire est $Fe^{3+}_{2.00}[Fe^{2+}_{2.02}Mg_{1.61}Fe^{3+}_{0.17}Mn^{2+}_{0.06}]_{\Sigma 3.86}(P_{1.02}O_4)(OH)_{11}(H_2O)$ sur une base de 16 atomes d'oxygène. La formule simplifiée est $Fe^{3+}_2(Fe^{2+},Mg)_4(PO_4)(OH)_{11}(H_2O)$. Une ébauche de la structure cristalline montre que la gladiusite est fortement maclée sur [001]. Ce minéral serait un produit de l'altération hydrothermale de la pyrrhotite et de la fluorapatite, les minéraux primaires porteurs de Fe et P dans la carbonatite à dolomite. Le nom du minéral signale la morphologie des cristaux, qui ressemble à une épée à double tranchant (*gladius*, en Latin) dans les images prises avec un microscope électronique à balayage.

(Traduit par la Rédaction)

Mots-clés: gladiusite, nouvelle espèce minérale, analyse à la microsonde électronique, spectre d'absorption infra-rouge, analyse thermogravimétrique, analyse thermique différentielle, phosphate hydroxylé et hydraté, Kovdor, Russie.

Introduction

During the last four decades, a large baddeleyite – apatite – magnetite deposit in the phoscorite–carbonatite complex of the Kovdor alkaline-ultramafic complex, Kola Peninsula, northwestern Russia, has been actively excavated. A new hydroxy-hydrated phosphate species, gladiusite, was discovered recently, exposed in hydrothermally altered veins of dolomite carbonatite in this complex. The mineral was named in accordance with the morphology of the crystals, which resemble double-edged swords (*gladius*, in Latin) in SEM images. Both the species and the name have been approved by the Commission on New Minerals and Mineral Names of the IMA. Holotype and other specimens of gladiusite are deposited at the Fersman Mineralogical Museum, Russian Academy of Sciences, Moscow; catalogue number 2310/1, and at the Geological Museum of the Institute of Geosciences, University of Oulu, Oulu, catalogue number 12182. Gladiusite is a rare mineral; only a few hundred mg are known to exist.

Occurrence

The igneous Kovdor ring complex occurs in the southwestern part of the Kola Peninsula (67°35' N, 30°20' E). Covering an area of 40.5 km^2, this body is the largest of its type in the Kola province of Paleozoic alkaline-ultramafic magmatism. The geology of this intrusion has been described in detail by Kukharenko *et al.* (1965), Ternovoi (1977), Kapustin (1980), Arzamastsev (1994), Kogarko *et al.* (1995) and Verhulst *et al.* (2000). The massif was emplaced into a Precambrian metamorphic sequence comprised mostly of amphibole–biotite gneiss (Belomorian suite), and is spatially controlled by the deep Kandalaksha fault (Kogarko *et al.* 1995). The intrusion has a concentric structure with subvertical contacts between adjacent units. An ultramafic core (olivinite, pyroxenite and diopside–olivine rocks) is surrounded by turjaite, melilitolite, phlogopite-bearing diopside–olivine rock, garnet – amphibole – monticellite rock, nepheline pyroxenite, phoscorite–carbonatite and carbonate–fluorapatite-cemented breccias, with outer zones of alkaline rocks (jacupirangite, ijolite–melteigite). A well-defined fenite zone surrounds the massif.

The phoscorite–carbonatite complex was emplaced into pyroxenites and ijolites, and is bordered by a semi-annular zone of a fine-grained apatite–forsterite metasomatic rock. The geology of the stock was described by Kukharenko *et al.* (1965), Ternovoi (1977), Kapustin (1980), Krasnova & Kopylova (1988) and Verhulst *et al.* (2000). Postmagmatic re-activation of the fault has caused extensive cataclasis, accompanied by an influx of hydrothermal fluids from the cooling phoscorite and carbonatite. As a result, the hydrothermal assemblages superimposed on the dolomite carbonatite contain a variety of rare minerals (Kukharenko *et al.* 1965, Kapustin 1980, Ivanyuk & Yakovenchuk 1997) dominated by hydroxy-hydrated (Mg, Fe^{2+})-phosphates (Table 1), eight of which occur at this locality only.

Gladiusite is confined to hydrothermal assemblages from vugs in cataclastic and mineralized dolomite carbonatite. The order of crystallization is as follows: primary pyrrhotite and fluorapatite → dolomite → pyrochlore → magnetite (type I) or *pyrite* → *rutile* → *ternovite-like phase* → *catapleiite* → *rimkorolgite* → *bobierrite* → *collinsite* → *juonniite* → *strontiowhitlockite* → *pyrrhotite* (type II) → gladiusite → *strontian collinsite* (0.76 *apfu* Sr, atoms per formula unit) → mag-

TABLE 1. HYDROUS Fe- AND Mg-PHOSPHATES FROM THE HYDROTHERMAL MINERAL ASSEMBLAGES RELATED TO DOLOMITE CARBONATITES OF THE KOVDOR MASSIF

Mineral	End-member formula	Range of Fe^{3+} *apfu*	Range of Fe^{2+} *apfu*	Range of Mg *apfu*	Reference
Collinsite	$Ca_2Mg(PO_4)_2(H_2O)_2$	–	0–0.28	0.69–1.02	unpublished
Bobierrite	$Mg_3(PO_4)_2(H_2O)_8$	tr.	0.07–0.53	2.50–2.99	unpublished
Barićite	$Mg_3(PO_4)_2(H_2O)_8$	0.03	1.17	1.72–1.74	unpublished
Vivianite	$Fe_3(PO_4)_2(H_2O)_8$	0.04–0.03	2.45–2.97	1.44–0.04	unpublished
Kovdorskite	$Mg_2(PO_4)(OH)(H_2O)_3$	tr.	0–0.21	2.0	Kapustin *et al.* (1980)
Bonshtedtite	$Na_3Fe^{2+}(PO_4)(CO_3)$	–	0.66	0.28	Khomyakov *et al.* (1982)
Girvasite	$NaCa_2Mg_3(PO_4)_2\{PO_2(OH)_2\}(CO_3)(OH)_2(H_2O)_4$	–	0.11–0.14	2.80–3.0	Britvin *et al.* (1990)
Strontiowhitlockite	$Sr_9Mg\{PO_3(OH)\}(PO_4)_6$	–	0.04–0.15	0.41–0.59	Britvin *et al.* (1991)
Rimkorolgite	$(Ba,Sr,Ca)Mg_5(PO_4)_4(H_2O)_8$	tr.	0.05–0.21	4.69–4.77	Britvin *et al.* (1995)
Krasnovite	$Ba(Al,Mg)(PO_4,CO_3)(OH)_2(H_2O)$	–	0.01	0.13	Britvin *et al.* (1996)
Juonniite	$CaMg(Sc,Mg)(PO_4)_2(OH)(H_2O)_4$	–	0.11	1.1–1.31	Liferovich *et al.* (1997)
Bakhchisaraitsevite	$\{Na_2(H_2O)_2\}\{Mg_5(H_2O)_5(PO_4)_4\}$	–	0.08–0.56	4.38–4.98	Liferovich *et al.* (2000)
Gladiusite	$Fe^{3+}{}_2(Fe^{2+},Mg)_4(PO_4)(OH)_{11}(H_2O)$	2.17	2.02	1.61	This study

Species in italics are known from the Kovdor hydrothermal assemblages only, tr. – traces.

netite-(type II) → chlorite → dolomite (the minerals associated with gladiusite are in italics). Gladiusite is not associated with other hydrous Fe-phosphates in these hydrothermal assemblages. Gladiusite is the first endogenic phosphate from this complex that has Fe^{3+} as a major cation (Table 1); vivianite and strengite occur in the upper horizons of the phoscorite–carbonatite complex and are exogenic (Kapustin 1980).

Physical and Optical Properties

Gladiusite occurs as acicular masses and as free-standing radiating clusters of arrow-head crystals (Fig. 1a); clusters do not exceed 2 mm in diameter. Gladiusite crystals (Fig. 1b) show subtly curved faces and a habit similar to a double-edged sword. Acicular crystals vary from 0.5 to 7 μm thick and from 10 to 500 μm long.

Gladiusite is dark green to almost black, opaque in aggregates and translucent only in thin needles, with an olive-green streak (in 10–12 h, the streak changes color to brownish red) and a vitreous luster. It does not fluoresce under long- or short-wave ultraviolet light. Gladiusite is soluble in hydrochloric acid (after some hours at room temperature). The mean Vickers hardness (VHN) of a dense aggregate of crystals is 300(25) (load 20 g, range 280–320 kg/mm^2; eight measurements were made on a polished block using a Mikromet II instrument), which corresponds approximately to a Mohs hardness of 4–4½. The density, 3.11(2) g/cm^3, was measured by flotation of gladiusite needles in a dilute Clerici–H_2O solution at 20°C; $D_{calc.}$ = 3.10(4) g/cm^3. Cleavage or parting was not observed. Gladiusite is brittle with an uneven fracture. It is biaxial negative, $c \parallel \gamma$, α 1.722(2), β 1.730(2), γ 1.737(2), $2V_{calc.}$ 86°. The dark color and strong pleochroism (*X* olive green, *Y* grayish blue, *Z* dark green with a blue tint, $X > Y > Z$) prevented complete determination of the optical properties and observation of the twinning that was later found during investigation of the crystal structure. A Gladstone–Dale calculation gave a compatibility index of –0.0062, superior (Mandarino 1981).

Crystallography

Preliminary precession photos of gladiusite needles suggest orthorhombic symmetry with possible space-groups *Pmmm, Pmm*2 or *P*222. However, crystal-structure determination (Sokolova *et al.* 2001) established the symmetry as monoclinic, space group $P2_1/n$, and showed the presence of pseudo-orthorhombic symmetry caused by extensive twinning. Unit-cell parameters, *a* 16.959(6), *b* 11.650(3), *c* 6.266(6) Å, β 90.00(5)°, *V* 1238(1) Å^3, *Z* = 4, were refined from X-ray powder-diffraction data (DRON–2.0 diffractometer, Cu*K*α radiation, graphite monochromator) using the indices derived from the crystal-structure determination (Table 2).

Chemical Analysis

Gladiusite was analyzed with a Cameca SX–50 electron microprobe operating in wavelength-dispersion mode with an operating voltage of 15 kV, specimen current of 10 nA, and counting times on peak and background of 20 and 10 s, respectively. The electron beam was focused to 5 μm, and the samples were moved during analysis to minimize decomposition. The following standards were used: forsterite (Mg), spessartine (Mn), marićite (Fe), fluorapatite (P) and titanite (Ti). The mean of 23 determinations is given in Table 3. The absence

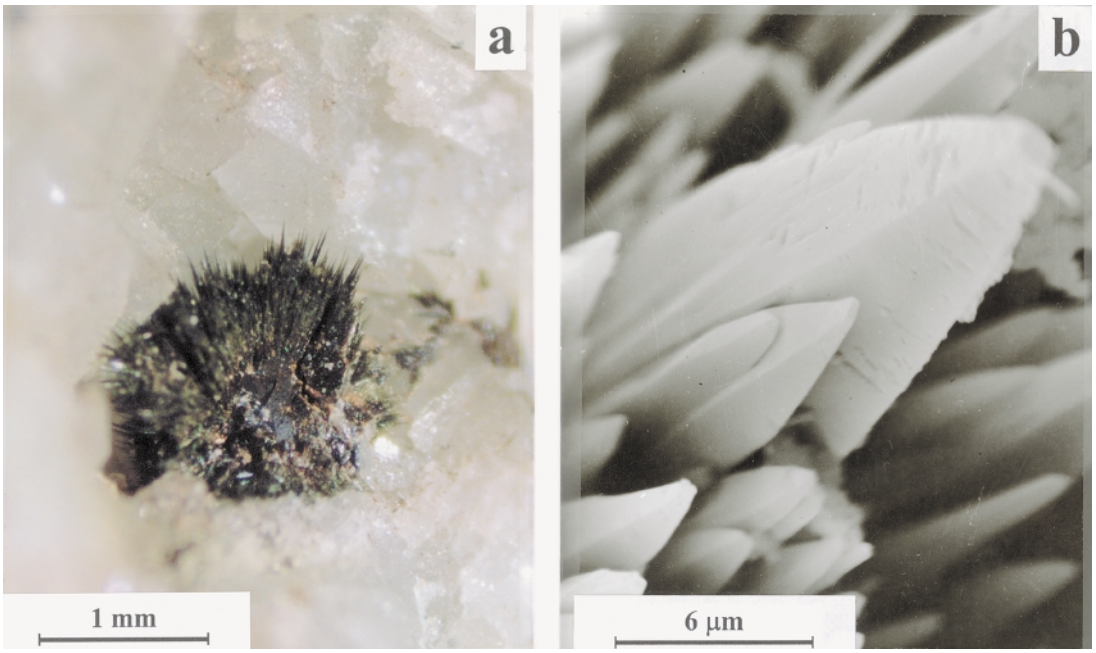

FIG. 1. (a) Photomicrograph of a cluster of gladiusite crystals within a vug in dolomite carbonatite. (b) SEM photomicrograph showing the morphology of the free-standing crystals of gladiusite.

of F was confirmed by a potentiometric technique (Li_3F electrode). Flame-emission spectra gave Be 0.005, Sc 0.01, Nb 0.02, Zr 0.05, V 0.003, and Ag 0.01 wt.%. Needles, used for study of all physical properties, tend to be slightly more magnesian than the dense aggregates of gladiusite. The presence of H (both OH and H_2O) was confirmed both by crystal-structure refinement and powder infrared-absorption. The oxidation state of iron was established by Mössbauer spectroscopy: 51% of the total Fe is Fe^{3+} (Sokolova *et al.* 2001). The empirical formula of gladiusite, calculated on the basis of O = 16 *apfu* (atoms per formula unit), is $Fe^{3+}_{2.0}[Fe^{2+}_{2.02}Mg_{1.61}Fe^{3+}_{0.17}Mn^{2+}_{0.06}]_{\Sigma 3.86}(P_{1.02}O_4)(OH)_{11.0}(H_2O)$; the general formula is $Fe^{3+}_2(Fe^{2+},Mg)_4(PO_4)(OH)_{11}(H_2O)$. The calculated value for H_2O, 20.18 wt.%, is close to the value determined by the Penfield method, 19.7 wt.%.

THERMOGRAVIMETRIC AND DIFFERENTIAL THERMAL ANALYSIS

Thermal curves for gladiusite (Fig. 2) were obtained in air using a derivatograph equipped with a Pt–PtRh thermocouple. The mean rate of heating was 6°C per minute from room temperature to 1050°C; α-alumina powder was used as a reference for DTA (Differential Thermal Analysis).

The exothermic effect at 200°C (DTA) (195°C, DTG) marks the beginning of oxidation of Fe^{2+} to Fe^{3+} (Dormann *et al.* 1982, Marincea *et al.* 1997). Loss of structurally bound H_2O is marked by an endothermic maximum at 270°C (DTA) and 265°C (DTG). Estimation of weight loss during the first stage of dehydration was complicated by overlap with the exothermic effect caused by the beginning of oxidation. The doublet of endothermic DTA peaks at 310°C and 400°C, respectively (305°C and 395°C on the TGA curve), marks a major loss of H_2O bound as OH groups. The total weight-loss (TGA) in the range 20–1050°C is 18.3 wt.%. After correction for oxidation of 25 wt.% FeO to Fe_2O_3, this loss is 21.1 wt.%, compared to a total H_2O content (determined with the Penfield method) of 19.7 wt.%. There are weak exothermic effects at 550 and 810°C on the DTA curve (Fig. 3). X-ray powder-diffraction of breakdown products indicates that gladiusite is stable up to 350°C; in the range 350–550°C, the X-ray-diffraction pattern is similar to that of magnetite; in the range 550–810°C, the material is almost amorphous, with some weak reflections attributable to α-$FePO_4$. At higher temperature, a hematite-like pattern was obtained.

INFRARED SPECTROSCOPY

An infrared-absorption spectrum of gladiusite (Fig. 3) was recorded between 400 and 3800 cm^{-1} using a UR–20 Carl Zeiss spectrometer and the KBr

TABLE 2. X-RAY POWDER-DIFFRACTION DATA FOR GLADIUSITE

I/I_o	d_{obs} (Å)	d_{calc} (Å)	*hkl*	I/I_o	d_{obs} (Å)	d_{calc} (Å)	*hkl*
53	9.61	9.60	110	9	2.383	2.393	$\bar{3}41$, 341
						2.372	710
77	6.87	6.86	210	3	2.313	2.313	422
89	5.83	5.83	020	4	2.237	2.237	720
16	5.51	5.51	120	4	2.210	2.209	540
29	5.09	5.09	310	3	2.155	2.154	350
100	4.805	4.802	220	7	2.119	2.119	800
62	3.787	3.786	130	1	2.094	2.098	$\bar{6}02$, 602
84	3.533	3.531	230	4	2.070	2.069	242, $\bar{2}42$
36	3.428	3.427	420	3	1.935	1.941	060
				〃	〃	1.929	160
15	3.380	3.391	500	9	1.893	1.893	260
〃	〃	3.362	$\bar{4}11$, 411				
11	3.254	3.256	510	14	1.860	1.862	740
				〃	〃	1.860	830
11	3.231	3.240	$\bar{1}31$, 131	1	1.791	1.792	920
7	3.168	3.200	330	5	1.714	1.718	$\bar{7}32$, 732
〃	〃	3.134	002	〃	〃	1.711	452, $\bar{4}52$
12	2.932	2.931	520	2	1.684	1.681	$\bar{8}22$, 822
10	2.888	2.890	$\bar{5}11$, 511	10	1.657	1.656	170
66	2.868	2.870	140	3	1.634	1.637	552, $\bar{5}52$
〃		2.864	430	〃	〃	1.633	270
31	2.829	2.826	600	4	1.600	1.601	$\bar{7}42$, 742
				〃	〃	1.601	$\bar{8}32$, 832
30	2.755	2.754	240	1	1.577	1.582	940
				〃	〃	1.580	271, $\bar{2}71$
				〃	〃	1.566	10.21
8	2.694	2.723	122	1	1.530	1.528	11.10
				〃	〃	1.527	$\bar{2}14$, 214
3	2.688	2.667	$\bar{3}12$, 312	1	1.488	1.490	11.20
				〃	〃	1.489	224, $\bar{2}24$
35	2.590	2.589	340	6	1.434	1.435	280
9	2.548	2.554	530	4	1.410	1.410	380
〃	〃	2.542	620				
17	2.414	2.414	132	4	1.374	1.376	$\bar{3}81$, 381
〃	〃	2.413	$\bar{1}32$	〃	〃	1.372	770
12	2.406	2.401	440				

DRON-2.0 diffractometer, graphite-monochromatized Cu*K*α radiation. Indexed on *a* 16.959(6), *b* 11.650(3), *c* 6.266(6) Å, β 90.00(5)°

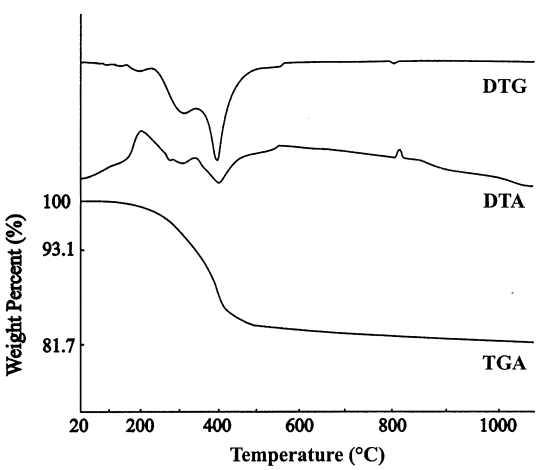

FIG. 2. Thermal analytical data for gladiusite.

pressed-disk technique. The strong absorption bands at 1020 and 1050 cm^{-1} are attributed to asymmetric stretching modes of the (PO_4) group, the bands at 560 and 528 cm^{-1} are due to bending modes of (PO_4), and the band at 962 cm^{-1} is a symmetric stretching mode of (PO_4). The bands at 3610 and 3172 cm^{-1} are O–H stretching vibrations; the band at 3485 cm^{-1} is an antisymmetric stretching mode of H_2O, and the band at 1628 cm^{-1} is the H–O–H bending vibration. Lower-frequency bands can be assigned to cation–O stretching-modes.

PARAGENESIS

The late hydroxy-hydrated minerals in carbonatites of the Kola alkaline province have been described as magmatic minerals. This view is misleading for the hydrous phosphates of vugs in mineralized dolomite carbonatite from the phoscorite–carbonatite complex of the Kovdor massif (Table 1). Most hydrous phosphates in this complex, including gladiusite, occur as free-standing crystals and clusters on water-clear crystals of late dolomite that coat fissures and cm- to dm-sized vugs in dolomite veins and adjacent rocks affected by epigenetic tectonism and hydrothermal activity. There is intensive dissolution and replacement of tabular crystals (0.1–5 cm) and aggregates of pyrrhotite, and of granular aggregates of fluorapatite by late Fe-rich minerals; these reactions are considered responsible for the release of Fe and P into the fluid phase. All consecutive stages of pyrrhotite alteration are observed (Figs. 4a, b):

1. Initial dissolution of pyrrhotite on mineral surfaces and cracks.

2. Intensive dissolution along the {0001} parting (Fig. 4a).

3. Crystallization of pyrite and formation of sooty aggregates of first-generation late magnetite (octahedra 0.1–300 μm in size, Fig. 4b). Fine-grained magnetite-I and pyrite are associated in some vugs. The newly

TABLE 3. CHEMICAL COMPOSITION (wt.%) AND UNIT FORMULA (*apfu*) OF GLADIUSITE

	Mean*	Range		
MgO	11.16(7)	8.8–15.6	P	1.02
MnO	0.78(2)	0.69–1.07		
+FeO	25.00(30)	46.47–55.39	Fe^{3+}	2.17
Fe_2O_3	29.90		Fe^{2+}	2.02
P_2O_5	12.46(15)	11.53–13.03	Mn	0.06
TiO_2	0.04(3)	0.00–0.12	Mg	1.61
†H_2O	20.18		□	0.14
Total	99.51		Σ	6.00
			OH	11
			H_2O	1

* mean of 23 determinations;
+ Fe^{3+}:Fe^{2+} ratio was obtained by Mössbauer spectroscopy;
† Calculated based on crystal-structure; 19.7 wt.% was obtained by the Penfield technique

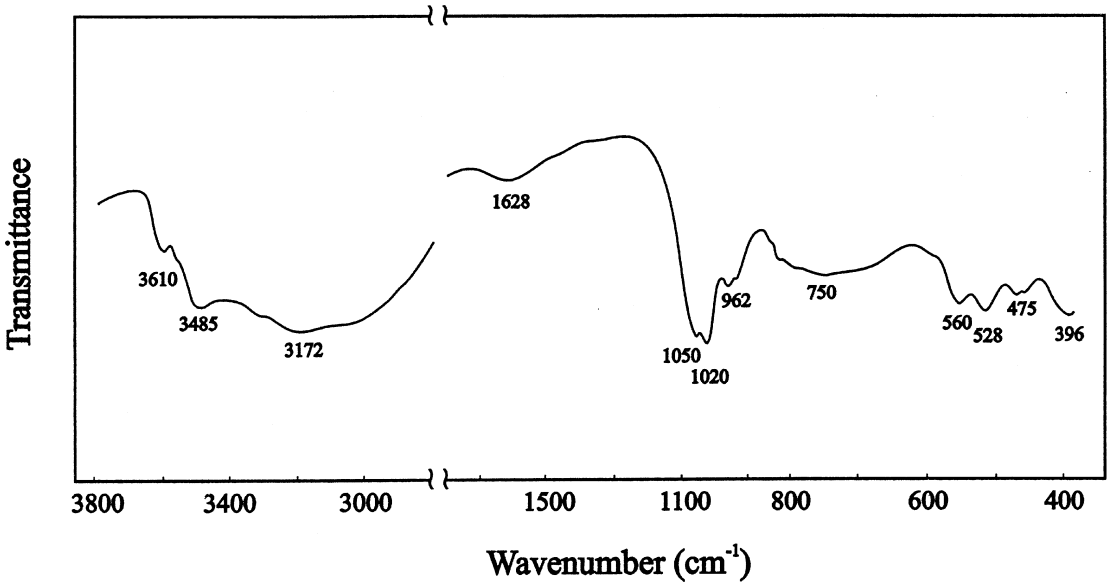

FIG. 3. The infrared spectrum of gladiusite.

formed Fe minerals do not occupy more than 50% of the volume of the primary pyrrhotite.

4. Complete alteration of pyrrhotite, resulting in formation of vugs. The dolomitic matrix was not corroded during leaching of primary pyrrhotite, and vugs commonly preserve the shape of the original pyrrhotite crystals and aggregates (Fig. 4).

5. Crystallization of hydrous phosphates (including gladiusite), chlorite, and local tiny late euhedral crystals of hydrothermal pyrrhotite. This hydrothermal pyrrhotite commonly shows some dissolution along its {0001} parting. In some vugs, needles of gladiusite are covered by fine radial aggregates of late magnetite (magnetite-II, Fig. 5).

The wide variety of minerals replacing primary pyrrhotite attests to extensive hydrothermal leaching in an open system. The variability of conditions was due to repeated influx of solutions and their interaction with the cataclastic rocks. Change of composition of hydrothermal solutions due to this interaction is clearly shown by the presence of bonshtedtite and nastrophite (sodium hydroxy-hydrated phosphates) in vugs in dolomite veins enclosed by nepheline pyroxenite (Khomyakov *et al.* 1982, Liferovich *et al*., in prep).

As indicated by the presence of several generations of magnetite, pyrite and late pyrrhotite, the fugacity of O_2 and H_2S varied greatly in the hydrothermal system. Because gladiusite occurs with pyrite and is not coeval with late magnetite, we propose that it formed under relatively high fugacity of H_2S in neutral solutions. Moreover, bakhchisaraitsevite does not occur with gladiusite (Liferovich *et al.* 2000). A synthetic phase, similar to bakhchisaraitsevite, was synthesized by Hallberg & Wadsten (1980) during leaching of iron monosulfide in reduced low-temperature aqueous media under alkaline conditions. Despite the fact that gladiusite and bakhchisaraitsevite occur in similar late assemblages, and both have H_2O, OH, Fe and Mg as principal constituents, the fact that they do not coexist suggests low-alkalinity conditions in the case of the gladiusite-forming hydrothermal solutions.

In turn, gladiusite is, in some cases, covered and replaced by fine radial aggregates of magnetite of type II (Figs. 5a, b). These pseudomorphs are widespread in the hydrothermal assemblages, and commonly are included in water-clear crystals of the latest dolomite. The presence of magnetite pseudomorphs after gladiusite in hydrothermal assemblages indicates that the range of stability of gladiusite, which forms in relatively reduced conditions, is rather limited. Siderite, a product of similar hydrothermal alteration of pyrrhotite in the carbonatite of the Khibina complex (Zaitsev *et al.* 1998), did not form during leaching of pyrrhotite in hydrothermal assemblages at Kovdor, indicating relatively low CO_2 fugacity. This observation may serve as a basis for estimation of the upper temperature of hydrothermal activity in the Kovdor phoscorite–carbonatite complex: it was below 270°C, which, according to Bulakh & Ivanikov (1984), is the point of decomposition of carbonatite-derived fluid into aqueous and gaseous CO_2 phases.

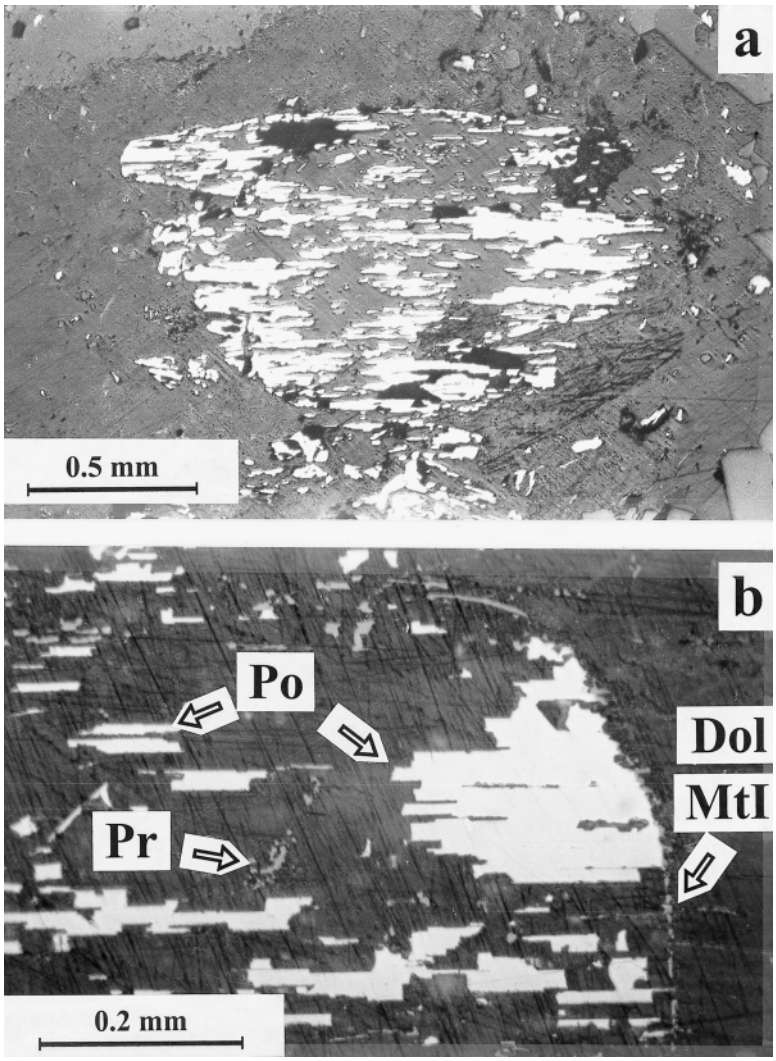

FIG. 4. (a,b) Intermediate stage of pyrrhotite leaching in cataclastic dolomite carbonatite and formation of vugs in carbonatite. The view is normal to the {0001} parting of the leached euhedral pyrrhotite crystal. Photomicrographs in reflected light. Po: pyrrhotite; Pr: pyrite; MtI: magnetite of the first hydrothermal generation; Dol: dolomite matrix of carbonatite; black: vugs after leached pyrrhotite.

Phosphorus is released *via* alteration of primary fluorapatite and replacement by aggregates of brown opaque hydroxylapatite; hydrothermal hydroxylapatite contains, on average, 2.0–2.5 wt.% less P_2O_5 than primary fluorapatite. This process occurs both in dolomite carbonatite and its host rock affected by hydrothermal activity along the reactivated fault-zone.

ACKNOWLEDGEMENTS

We are grateful to Dr. Catherine McCammon (Bayerisches Geoinstitut, Universität Bayreuth) for the Mössbauer study of gladiusite. Arnim Walter and Tim Jokela Jr. ("Element 51") are thanked for the color photomicrographs. The authors thank E.A. Krasovsky and A.N. Putilov from the Geological Department of the management staff of Kovdorsky GOK joint-stock com-

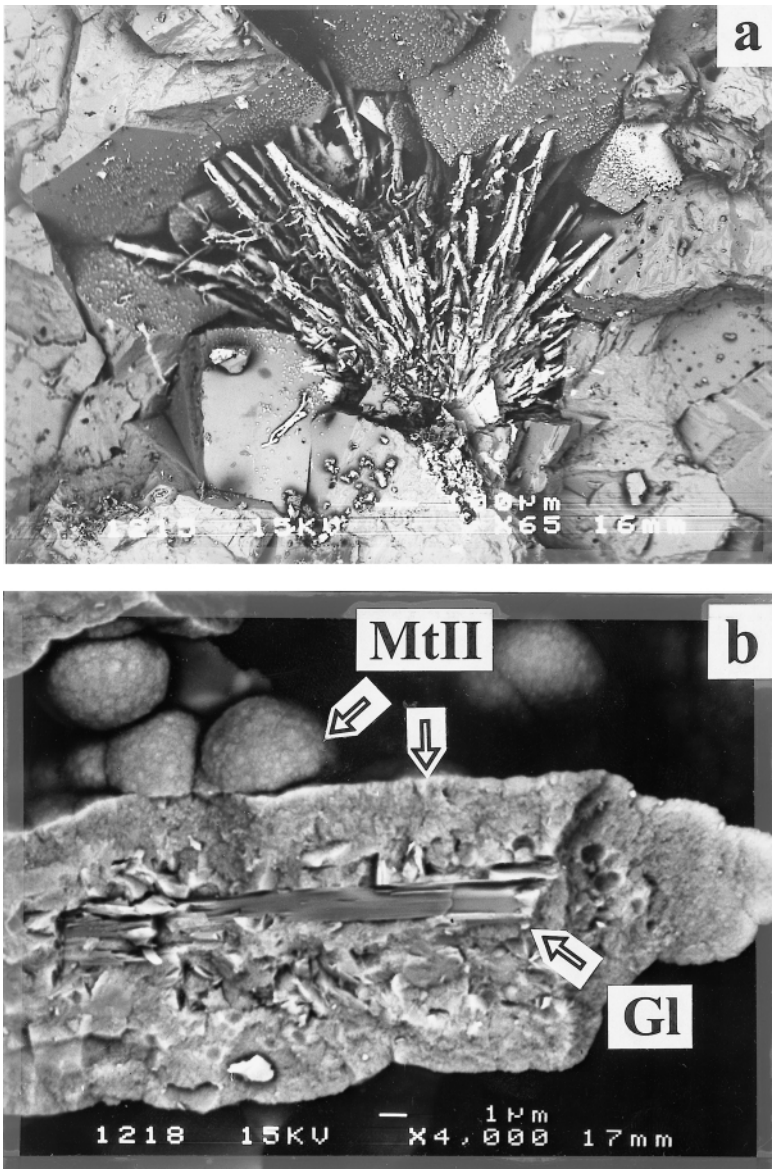

FIG. 5. Replacement of gladiusite (Gl) by hydrothermal magnetite-II (MtII). (a) Magnetite aggregate, morphologically similar to gladiusite aggregates (Fig. 1a). (b) Corroded and crushed gladiusite crystals covered and partially replaced by fine radial aggregates of magnetite-II.

pany for their help during field work. We are grateful to L.I. Konstantinova, A.E. Bykova, M.F. Lyalina, and Dr. V.Ya. Kuznetsov (Geological Institute and ICHTRERM, Kola Science Center, Russian Academy of Sciences), O. Taikina-aho, R. Peura and E. Hiltola (Institute of Electron Optics, University of Oulu) for their assistance, and Dr. N.V. Chukanov (Institute of Chemical Physics, Chernogolovka, Moscow District) for the IR-spectrum. Helpful comments were provided by Drs. Gunnar Raade, Joe Mandarino, the ubiquitous Anonymous and the omnipotent Bob Martin. RPL and YAP benefitted from the INTAS project 97–0722, RPL was also supported by the Academy of Finland. FCH was supported by Natural Sciences and Engineering Re-

search Council of Canada Major Equipment, Major-Facilities Access and Research grants.

REFERENCES

ARZAMASTSEV, A.A. (1994): *Unique Palaeozoic Intrusions of the Kola Peninsula*. Kola Science Center Press, Apatity, Russia.

BRITVIN, S.N., PAKHOMOVSKY, YA.A. & BOGDANOVA, A.N. (1996): Krasnovite, $Ba(Al,Mg)[PO_4,CO_3](OH)_2 \cdot H_2O$, a new mineral. *Zap. Vser. Mineral. Obshchest.* **125**(3), 110–112 (in Russ.).

_____, _____, _____, KHOMYAKOV, A.P. & KRASNOVA, N.I. (1995): Rimkorolgite $(Mg,Mn)_5(Ba,Sr,Ca)[PO_4]_4$ß8$H_2O$ – a new mineral from the Kovdor iron deposit, Kola peninsula. *Zap. Vser. Mineral. Obshchest.* **124**(1), 90-95 (in Russ.).

_____, _____, _____ & SKIBA, V.I. (1991): Strontiowhitlockite, $Sr_9Mg(PO_3OH)(PO_4)_6$, a new mineral species from the Kovdor deposit, Kola peninsula, USSR. *Can. Mineral.* **29**, 87-93.

_____, _____, _____ & SOKOLOVA, E.V. (1990): Girvasite – a new carbonate–phosphate of sodium, calcium and magnesium from carbonatites of Kovdor massif (Kola peninsula). *Mineral. Zh.* **12**(3), 79-83 (in Russ.).

BULAKH, A.G. & IVANIKOV, V.V. (1984): *The Problems of Mineralogy and Petrology of Carbonatites.* Univ. Leningrad Press, Leningrad, Russia (in Russ.).

DORMANN, J.L., GASPÉRIN, M. & POULLEN, J.-F. (1982): Étude structurale de la séquence d'oxydation de la vivianite, $Fe^{2+}(PO_4)_3 \cdot 8H_2O$. *Bull. Minéral.* **105**, 147-160.

HALLBERG, R.O. & WADSTEN, T. (1980): Crystal data of a new phosphate compound from microbial experiments on iron sulfide mineralization. *Am. Mineral.* **65**, 200-204.

IVANYUK, G.YU. & YAKOVENCHUK, K.N. (1997): *Minerals of the Kovdor Massif*. Kovdorsky GOK Joint-Stock Company & Kola Science Center, Russian Academy of Sciences, Apatity, Russia.

KAPUSTIN, YU.L. (1980): *Mineralogy of Carbonatites*. Amerind Publishing, New Delhi, India.

_____, BYKOVA, A.V. & PUDOVKINA, Z.V. (1980): Kovdorskite, a new mineral. *Zap. Vses. Mineral. Obshchest.* **109**(3), 341-347 (in Russ.).

KHOMYAKOV, A.P., ALEXANDROV, V.B., KRASNOVA, N.I., ERMILOV, V.V. & SMOL'YANINOVA, N.N. (1982): Bonshtedtite $Na_3Fe(PO_4)(CO_3)$ – a new mineral. *Zap. Vses. Mineral. Obshchest.* **111**(4), 486-490 (in Russ.).

KOGARKO, L.N., KONONOVA, V.A., ORLOVA, M.P. & WOOLLEY, A.R. (1995): *Alkaline Rocks and Carbonatites of the World. 2. Former USSR*. Chapman & Hall, London, U.K.

KRASNOVA, N.I. & KOPYLOVA, L.N. (1988): The geologic basis for mineral-technological mapping at the Kovdor ore deposit. *Int. Geol. Rev.* **30**, 307-319.

KUKHARENKO, A.A., ORLOVA, M.P., BULAKH, A.G., BAGDASAROV, E.A., RIMSKAYA-KORSAKOVA, O.M., NEFEDOV, E.I., IL'INSKII, G.A., SERGEEV, A.S. & ABAKUMOVA, N.B. (1965): *The Caledonian Complex of the Ultrabasic Alkaline Rocks and Carbonatites of the Kola Peninsula and Northern Karelia*. Nauka, Moscow, Russia (in Russ.).

LIFEROVICH, R.P., PAKHOMOVSKY, YA.A., YAKUBOVICH, O.V., MASSA, W., LAAJOKI, K., GEHÖR, S., BOGDANOVA, A.N. & SOROKHTINA, N.V. (2000): Bakhchisaraitsevite, $Na_2Mg_5[PO_4]_4 \cdot 7H_2O$, a new mineral from hydrothermal assemblages related to phoscorite–carbonatite complex of the Kovdor massif, Russia. *Neues Jahrb. Mineral., Monatsh.* (in press).

_____, YAKOVENCHUK, V.N., PAKHOMOVSKY, YA.A., BOGDANOVA, A.N. & BRITVIN, S.N. (1997): Juonniite – a new mineral of scandium in calcite-dolomite carbonatite from Kovdor massif. *Zap. Vser. Mineral. Obshchest.* **126**(4), 80-88 (in Russ.).

MANDARINO, J.A. (1981): The Gladstone-Dale relationship. IV. The compatibility concept and its application. *Can. Mineral.* **19**, 441-450.

MARINCEA, S., CONSTANTINESCU, E. & LADRIERI, J. (1997): Relatively unoxidized vivianite in limnic coal from Capeni, Baraolt Basin, Romania. *Can. Mineral.* **35**, 713-722.

SOKOLOVA, E., HAWTHORNE, F.C., MCCAMMON, C. & LIFEROVICH, R.P. (2001): The crystal structure of gladiusite, $Fe^{3+}{}_2Fe^{2+}{}_4(PO_4)(OH)_{11}(H_2O)$. *Can. Mineral.* **39** (in press).

TERNOVOI, V.I. (1977): *Carbonatite Massifs and their Ores*. Univ. Leningrad Press, Leningrad, Russia (in Russ.).

VERHULST, A., BALAGANSKAYA, E., KIRNARSKY, Y. & DEMAIFFE, D. (2000): Petrological and geochemical (trace elements and Sr/Nd isotopes) characteristics of the Paleozoic Kovdor ultramafic, alkaline and carbonatite intrusion (Kola peninsula, NW Russia). *Lithos* **51**, 1-25.

ZAITSEV, A.N., SINAI, YU.M., SHAKHMURADYAN, A.R. & LEPEKHINA, E.N. (1998): Association of pyrrhotite and pyrite in carbonatite series rock of Khibina alkaline massif. *Zap. Vser. Mineral. Obshchest.* **127**(4), 110–119 (in Russ.).

Received July 17, 2000, revised manuscript accepted October 29, 2000.